IEEE Access
Multidisciplinary | Rapid Review | Open Access Journal

Received May 10, 2017, accepted May 31, 2017, date of publication June 7, 2017, date of current version June 27, 2017.

Digital Object Identifier 10.1109/ACCESS.2017.2712614

Digital Self-Interference Cancellation Based on Independent Component Analysis for Co-Time Co-frequency Full-Duplex Communication Systems

JIONG LI, (Student Member, IEEE), HANG ZHANG, (Member, IEEE), AND MENGLAN FAN, (Member, IEEE)

College of Communications and Engineering, PLA University of Science and Technology, Nanjing 210007, China

Corresponding author: Jiong Li (lij_2015@126.com)

This work was supported by the Natural Science Foundations of China under Grant 61671475).

ABSTRACT Co-frequency and co-time full-duplex (CCFD) technique claims to be the most potential duplex scheme for the next generation system, since it can double the spectral efficiency. The challenge of CCFD wireless communication systems lies in mitigating the self-interference (SI). In this paper, we focus on the digital SI cancellation (SIC) in the CCFD systems. The performance of the traditional digital cancellation techniques is mainly limited by the nonlinearity of the components of local transmitter. Aiming at the issue an auxiliary receive chain is employed in this paper. In addition, by exploiting the independence between signal of interest and self-interfering signal, two digital SIC algorithms based on independent component analysis are developed for two application scenarios of the CCFD technique, i.e., CCFD satellite communication systems and ground CCFD communication systems. Instead of achieving cancellation by reconstructing self-interfering signal in other works, the proposed algorithms extract desired signal from the received signal. Simulation results indicate that the proposed algorithms outperform conventional least square digital cancellation method.

INDEX TERMS Co-frequency and co-time full-duplex (CCFD), independent component analysis (ICA), self-interference cancellation (SIC).

I. INTRODUCTION

The design of a wireless communication system has been limited by the assumption that radios must either transmit or receive on the same channel, but not simultaneously (i.e., in half duplex (HD) mode) [1]. This leads to significant loss of spectrum efficiency. Recently, a wave of co-frequency and co-time full duplex (CCFD) research breaks out since it has great potential for improving spectra efficiency. With a CCFD communication system, radios can transmit and receive signals on the same channel simultaneously and thus, theoretically, can double the spectrum efficiency. References [2], [3] studied the potential applications of CCFD in 5G networks to assist in achieving the goal of improving throughput 1000 times compared with 4G networks. Reference [4] exploited CCFD for device-to-device (D2D) communications in heterogeneous networks. Reference [5] proposed a new design paradigm for enhancing spectrum usage using CCFD in cognitive radio. Reference [6] addressed the challenges of transceiver in mobile CCFD devices. All the literature [2]–[6] emphasized that the key issue in implementing CCFD is self-interference (SI). When a CCFD radio works, some of its transmission energy is transmitted to its own receiver. Due to the fact that the undesired self-interfering signal is generated locally and the limitation of the user equipment size, the undesired signal is billions of times stronger than the signal of interest. For instance, in Wi-Fi systems, the average transmission power and noise floor are around 20dBm and −90dBm respectively, that is, a total of 110dB SI suppression is required to ensure the proper operation of CCFD system [7]. For Long Term Evolution (LTE) system, the signals propagate over longer ranges such that a larger gap is generated between transmitter power and sensitivity, which requires a higher ability of SI suppression at around 123dB.

In case that the SI suppression capability does not reach the requirement, the residual self-interfering signal will negatively affect the throughput.

Since the signal is transmitted by the CCFD radio, the self-interfering signal is known to its own receiver. Intuitively, it should be relatively straightforward to subtract the self-interfering signal from the received signal. However, it is far from that. Although the sender knows the clean digital baseband signal, the signal undergoes many unwanted impairments in transmit chain. The impairments may include both linear and nonlinear distortion (e.g., non-ideal analog components produce cubic or high-order distortions, such as power amplifiers (PA)), additional noise (e.g., analog circuits create transmitter noise), oscillator offset, and so on. Consequently, the received self-interfering signal consists of the linear and nonlinear component of the ideal transmitted signal and unknown noise. Obviously, it is not appropriate to directly subtract the self-interfering signal in a ''known'' baseband version from the received signal irrespective of these distortion factors.

Recently, several research groups [6]–[15] have considered the problem of SI suppression in CCFD system both in academic research and engineering practice. Some research results [9]–[15] have shown that CCFD radios are implementable in lab conditions. In the latest literature [9], it also has been shown that the designed CCFD system prototype achieves about 1.9 times higher throughput than a HD system. Although some exciting results have been achieved in laboratory environment, as mentioned in [9], the degree of SI cancellation (SIC) is still the key factor limiting the practicality of full-duplex practicality. In this paper, we will further explore the SIC for CCFD systems.

The methods of SIC in CCFD system can be divided into two categories: namely passive and active SIC. Passive methods rely on the directional SI suppression and antenna separation [3], [8], to increase the isolation between the transmit and receiving antennas, and hence reduce the power of the self-interfering signal. 25-40dB interference suppression ratio can be obtained through passive methods [8]–[10], [12]. In active methods, the self-interfering signal is reconstructed and subtracted from received signal. According to the different signal processing domain (analog or digital domain) where the SI is suppressed, the active methods can be divided into analog and digital cancellation techniques, which are always before and after the analog-to-digital converter (ADC) respectively.

In general, analog cancellation is implemented at radio frequency (RF) domain to prevent the receiver components saturating [8], [9], [13], [14], [16]–[18]. If the input signal-to-interference ratio (SIR) of ADC is lower than a determined value, the signal of interest will be distorted seriously caused by the quantization error of the ADC. Analog cancellations also can be implemented at baseband [19]. However, considering commercial issue and the fact that the baseband analog cancellation (BAC) gains are not clear, BAC techniques are not common. Limited by analog devices, analog cancellation techniques can only provide 18-40dB suppression [6], [8], [9]. Although a large amount (43-80dB) of SI has been suppressed by passive SIC and active analog cancellation techniques, there are still tens dB SI need to be further processed in digital domain. Compared with analog cancellation techniques, digital cancellation is more flexible, which can estimate SI channel and reconstruct self-interfering signal conveniently.

In this paper, we investigate the SIC in digital domain. As reported in [16], [17], [20], and [22], the most of analog cancellation methods can only suppress the line of sight (LOS) SI. To further eliminate self-interference, digital cancellation is implemented to deal with the non-LOS components. The multipath SI channel can be modeled as finite-impulse-response (FIR) filter. In [23], the SI channel coefficients are estimated in frequency domain. Reference [24] proposed a two-step algorithm based on Least Square (LS) to estimate SI channel. Reference [25] investigated the SIC technique for CCFD relays and multiple-in-multiple-out (MIMO) transceiver using LS methods as well. However, in most of these methods, the non-idealities of analog/RF circuit have not been considered. Zheng *et al.* [26] modeled the transmitter non-idealities as white noise in the context of cognitive radios. The effect of phase noise from oscillators on cancellation is studied in [20], [25], [27], and [28]. In these studies, it was shown that the phase noise can potentially limit the amount of achievable SIC and using identical oscillator for transmitter and receiver can reduce the impact of phase noise (about 25dB gains can be obtained from SIC). However, as discussed in [22], the effects of phase noise are low enough and are no longer the bottleneck of the system. References [7], [29] investigated comprehension distortion calculations including nonlinear distortion, I/Q mismatch and other things. The findings in [7] and [29]–[32] indicate that the transmitter PA can significantly contribute to the self-interfering signal and form a significant bottleneck in CCFD radio devices.

Thus, in this work, we focus on the achievable SIC at digital processing stage of receiver with full consideration of nonlinear distortion at transmit chain. In addition, since an expected SIC is carried out in the digital domain, another main component that can degrade the signal-to-interference-noise ratio (SINR) at detector input of receiver is the quantitation error of the ADC. We also analyze the effect of the quantization error for the performance of CCFD receiver. Specifically, the impact of analog impairments at transmitter is introduced, and to avoid the effects of these impairments at active SIC stages (both in analog and digital domain) in receiver, a SIC scheme based on an auxiliary receive chain to copy self-interfering signal respectively in RF and digital domains is employed [22]. In most literature of self-interference cancellation (SIC) in full duplex system, SIC is achieved based on LS method. In this paper, by introducing an auxiliary receive chain and after some formula derivation, we transfer the SIC problem into blind source separation (BSS) [33], [34] problem, and the independence between the self-interfering signal and the desired

signal is effectively utilized. In addition, we propose two SIC algorithms based on independent component analysis (ICA) [35], [36] for two different self-interference channel models, respectively, and the simulation results show that the performance of the proposed algorithms is much better than LS-based SIC methods. The content of this paper provides a new and better way to achieve baseband SIC in theory. Moreover, careful screening shows that ICA method has never been applied to SIC in full duplex system before.

The rest of this paper is organized as follows. In Section II, we present the CCFD wireless communication system model, and the signal model follows. The proposed methods for self-interference cancellation of CCFD satellite communication systems and ground CCFD wireless communication systems are given in Section III. In Section IV, the performance of the proposed methods under different scenarios is analyzed. Finally, Section V concludes this paper.

II. CCFD WIRELESS COMMUNICATION SYSTEM MODEL

In this section, the CCFD transceiver principle is introduced from the view of SIC problem. According to the different applications of CCFD, channel models are analyzed. And then, the signal models are given considering the impact of transceiver impairments and the effects of channel.

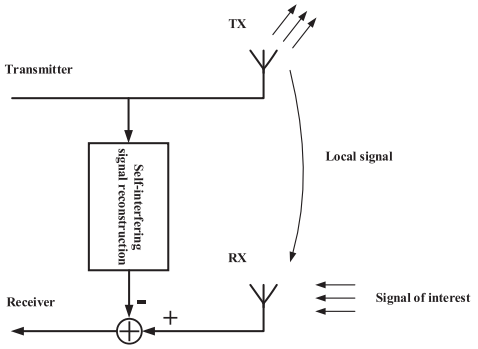

FIGURE 1. Basic configuration of traditional CCFD device: transmitter and receiver work on the same center frequency at the same time and a self-interfering reconstruction block aids to achieve SIC.

A. CCFD TRANSCEIVER PRINCIPLE

The CCFD communication devices work on the same center frequency at the transmitter and receiver at the same time, as shown in Fig. 1. The mixing signal heard by the CCFD device includes three components: signal of interest (transmitted by other device), local signal (i.e., self-interfering signal comes from its own transmitter) and noise. Obviously, the SIC is necessary for proper decoding the weak signal of interest

Fig.2 shows a detailed block diagram for our digital SIC approach based on a new CCFD transceiver architecture. The new transceiver consists of an ordinary transmitter and a new receiver. The new receiver consists of an ordinary receive chain, a RF SIC module and an auxiliary receive chain used for extracting desired signal. In the transmit chain, source signal can be modulated with arbitrary modulation mode, and then up-converted to the radio frequency. The RF signal is then filtered, power amplified and transmitted. The power splitter assigns some energy of the amplified signal as reference signal to the RF SIC module and the auxiliary receive chain. Since the input signal power of the auxiliary receive chain is controlled by the power splitter, the low noise amplifier (LNA) is no longer needed in the auxiliary receive chain. The reference signal at input of the RF SIC module helps to cancel RF LOS interference like in [9], [10], and [16]. The auxiliary receive chain and the ordinary receive chain share the same local oscillator (LO). The reference signal at input of the auxiliary receive chain and the residual signal after RF SCI stage are down-converted to baseband through the two receive chains respectively, then the desired signal is extracted from these two baseband signals.

Single antenna architecture with a circulator also can be employed in the transceiver. However, since the number of antennas is not the main issue of this paper, for convenience, we take the architecture based on two antennas for example.

B. SELF-INTERFERENCE CHANNEL MODELING

In this paper, two SI channel models are in consideration, i.e., SI channel only has LOS component and SI channel has LOS and non-LOS components. Two application scenarios are taken into consideration, satellite communication systems and ground communication systems.

In general, the self-interfering signal consists of two main components: LOS component comes from transmitting antenna directly and non-LOS component comes from the reflections of the transmit antenna. For CCFD satellite communication systems, the SI channel of satellite terminals only has LOS component since the satellite is in the vast outer space without any reflector around it. While for the ground terminals of satellite communications, according to the working frequency range, the SI channel can be multipath or only have LOS component. For example, fixed terminals working on C-band frequency have narrow beams, so almost no multipath components exist in SI channel (SI channel only has LOS component), while for mobile satellite communication terminals working on UHF-band, the beams are wide such that multipath components exist. In ground wireless communication systems, the non-LOS components account for a considerable part of the self-interfering signal. The channel could be modeled as a FIR filter.

C. SIGNAL MODELS WITH COMPONENT IMPAIRMENTS

In this paper, the main impairments of the CCFD transceiver are considered. Specifically, the PA nonlinearity of the transmitter, ADC quantization noise and receiver Gaussian noise. We assume that other components do not have nonlinearity due to the fact that power efficiency is not critical for them except for the PA. I/Q imbalances may also exist at the I/Q mixer in transmit and receive chains [37]. However, according to the current device accuracy, the image rejection ratio

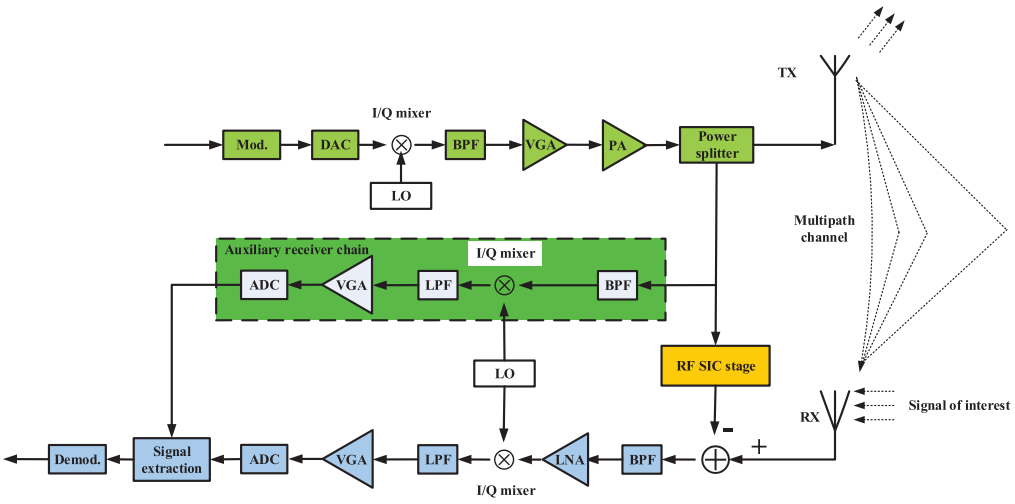

FIGURE 2. Detailed block diagram for the proposed digital SIC approach.

can reach 60-80 dB at 500MHz-6GHz carrier frequency [38], so the impact of I/Q imbalance could be neglected. For ease of analysis, baseband equivalent signal models are employed in the following.

The complex baseband signal which is transmitted after digital to analog convertor (DAC) is denoted by $x(t)$. Some imbalance between I and Q branches take place at I/Q mixer [37], and the signal at the output of transmitter I/Q mixer can be written as

$$x_T^{IQ}(t) = g_{1,T}x(t) + g_{2,T}x^*(t) \tag{1}$$

where $(\bullet)^*$ denotes the complex conjugate, $g_{1,T}$ and $g_{2,T}$ are the gains for the direct and image components respectively. Before transmission, the signal is filtered with a bandpass filter (BPF) and then amplified with a nonlinear PA. In this paper, we assume that all filters are sufficiently flat in band. For any nonlinear operation, the output signal can be modeled as a polynomial function of input signal [39]. In practice, typically, the nonlinearity is characterized by the third order intercept point [40], and the signal at the output of PA can be written as [41]

$$x_T^{PA}(t) = \alpha_0 x_T^{IQ}(t) + \alpha_1 x_T^{IQ}(t)\left|x_T^{IQ}(t)\right|^2 \tag{2}$$

where α_0 and α_1 denote the linear gain and the gain of third order component respectively.

Next, the amplified signal is transmitted and couples back to the receiving antenna, and thus SI is generated. The received signal at the input of the ordinary receive chain is

$$r_R^{RF}(t) = h_{SI}(t) \otimes x_T^{PA}(t) + h_{soi}(t) \otimes s(t) + n_{in}(t) \tag{3}$$

where $\otimes$ indicates the convolution operation, $s(t)$ is the signal of interest, $h_{SI}(t)$ and $h_{soi}(t)$ are the responses of SI and signal of interest channels, $n_{in}(t)$ denotes thermal noise. To avoid the saturation of LNA, RF SIC is performed (where could be a single tap filter to suppress the LOS component [9], [10] or a multiple taps filter to suppress LOS and non-LOS components [42]). After RF SIC, the residual signal is

$$r_R^{\mathrm{Re}\,s}(t) = f(t) \otimes x_T^{PA}(t) + h_{soi}(t) \otimes s(t) + n_{in}(t) \tag{4}$$

where $f(t)$ is the residual channel response of SI channel after RF SIC stage. A LNA is following to amplify the residual signal, and the output of the LNA can be written as

$$r_R^{LNA}(t) = g_{LNA} r_R^{\mathrm{Re}\,s}(t) + n_{LNA}(t) \tag{5}$$

where g_{LNA} is the gain of the LNA, $n_{LNA}(t)$ is the noise caused by LNA. Like the transmitter, some I/Q imbalance also happens at receiver I/Q mixer [37], and the down-converted signal can be written as

$$r_R^{IQ}(t) = g_{1,R} r_R^{LNA}(t) + g_{2,R}\left(r_R^{LNA}(t)\right)^* \tag{6}$$

where $g_{1,R}$ and $g_{2,R}$ are the gains for the direct and image components respectively. As previously analyzed, the image rejection ratio of the devices can reach a rather high level, so the image components can be neglected. Finally, the variable gain amplifier (VGA) is used to adjust the power of $r_R^{IQ}(t)$ to match the input voltage range of ADC, and then digitize the signal. The digitized signal can be expressed as

$$y(nT_s) = g_{VGA} r_R^{IQ}(nT_s) + n_{ADC}(nT_s) \tag{7}$$

where T_s indicates the sampling interval, g_{VGA} is the gain of the VGA, $n_{ADC}(nT_s)$ is the quantization noise. For brevity, T_s is dropped in the rest. A complete equation for $y(n)$ can be derived by combining (4) to (7)

$$\begin{aligned} y(n) = {} & f_{SI}(n) \otimes x_T^{PA}(n) + f_{SOI}(n) \otimes s(n) \\ & + n_a(n) + n_{ADC}(n) \end{aligned} \tag{8}$$

where

$$f_{SI}(n) = g_{VGA} g_{1,R} g_{LNA} f(n) \tag{9}$$

$$f_{SOI}(n) = g_{VGA} g_{1,R} g_{LNA} h_{soi}(n) \tag{10}$$

$$n_a(n) = g_{VGA} g_{1,R} g_{LNA} n_{in}(n) + g_{VGA} g_{1,R} n_{LNA}(n) \tag{11}$$

and the signal to noise ratio (SNR) of the ADC is defined as [43]

$$SNR_{ADC} = 10^{(6.02b+4.76-PAPR)/10} \tag{12}$$

where b indicates the number of quantization bit of the ADC, PAPR denotes the peak-to-average-power ratio (PAPR) of the input signal of the ADC in dB.

The baseband version of auxiliary receive chain is

$$x_{Aux}(n) = \varepsilon x_T^{PA}(n) + n_{ADC}^{Aux}(n) \tag{13}$$

where $\varepsilon = \varepsilon_0 g_{VGA} g_{1,R}$, ε_0 is the power division factor of the power splitter, $n_{ADC}^{Aux}(n)$ is the quantization noise of the ADC in auxiliary receive chain.

III. BASEBAND DIGITAL SIC BASED ON ICA FOR CCFD COMMUNICATIONS

In this section, we introduce two digital SIC algorithms, which can be used in CCFD satellite communication systems and ground communication systems, respectively, based on ICA method using the reference signal from the output of the transmitter PA.

A. DIGITAL SIC BASED ON ICA FOR ONLY LOS COMPONENT EXISTING IN SI CHANNEL

In this case, only LOS component exists in self-interfering signal. The signal model of the two receive chain can be written as

$$\mathbf{R}(n) = \mathbf{M}\begin{bmatrix} x_T^{PA}(n) \\ s(n) \end{bmatrix} + \begin{bmatrix} \xi(n) \\ n_{ADC}^{Aux}(n) \end{bmatrix} \tag{14}$$

where $\xi(n) = n_a(n) + n_{ADC}(n)$, $\mathbf{R}(n) = \left[y(n)\ x_{Aux}(n)\right]^T$ and $\mathbf{M} = \begin{bmatrix} f_{SI} & f_{SOI} \\ \varepsilon & 0 \end{bmatrix}$

The aim of ICA-based source separation method is to search for a demixing matrix $\mathbf{B}$, and the linear transformation of the two receive signals are used to estimate source signals. It can be expressed as

$$\mathbf{E}(n) = \mathbf{B}\mathbf{R}(n) \tag{15}$$

where $\mathbf{E}(n)$ is the estimation of $\left[x_T^{PA}(n)\ s(n)\right]^T$. Ideally, when no noise exists in (14), $\mathbf{B}$ is equal to the inverse of the matrix $\mathbf{M}$, but it is hard to achieve. So, we define the estimation is success when $\mathbf{BM}$ is a generalized permutation matrix (i.e., only one non-zero element exists in each row and each column in the matrix).

A fast fixed-point ICA algorithm [35] is adopted as follows.

1) Prewhitening by EVD

The covariance matrix of the received data $\mathbf{R}(n)$ is denoted $\mathbf{C} = E\left[\mathbf{R}(n)\mathbf{R}^H(n)\right]$, where $E[\bullet]$ denotes the expected value. The eigenvalue decomposition (EVG) of $\mathbf{C}$ is $\mathbf{C} = \mathbf{UDU}^H$, where $\mathbf{U}$ is a 2×2 conjugate matrix, and $\mathbf{D} = \begin{bmatrix} d_1 & 0 \\ 0 & d_2 \end{bmatrix}$ is the eigenvalue matrix. The whitening process can be written as

$$\mathbf{Z}(n) = \mathbf{D}^{-\frac{1}{2}}\mathbf{U}^H\mathbf{R}(n) = \mathbf{A}\begin{bmatrix} x_T^{PA}(n) \\ s(n) \end{bmatrix} + \mathbf{D}^{-\frac{1}{2}}\mathbf{U}^H\begin{bmatrix} \xi(n) \\ n_{ADC}^{Aux}(n) \end{bmatrix} \tag{16}$$

where $\mathbf{A} = \mathbf{D}^{-\frac{1}{2}}\mathbf{U}^H\mathbf{M}$ is whitening-mixing matrix.

2) ICA-based separation of received signals The ICA-based separation algorithm is to search for an orthogonal matrix $\mathbf{W} = [\mathbf{w}_1, \mathbf{w}_2]$ to make the global matrix $\mathbf{G} = \mathbf{W}^H\mathbf{A}$ is a generalized permutation matrix. Following [35], the first orthogonal vector $\mathbf{w}_1$ can be estimated as follows:

a) Initialize $\mathbf{w}_1$ with a random unit-norm vector.

b) Update $\mathbf{w}_1$

$$\begin{aligned} \mathbf{w}_1 = {} & E\left\{\mathbf{Z}(n)\left(\mathbf{w}_1^H\mathbf{Z}(n)\right)^* g\left(\left|\mathbf{w}_1^H\mathbf{Z}(n)\right|^2\right)\right\} \\ & - E\left\{g\left(\left|\mathbf{w}_1^H\mathbf{Z}(n)\right|^2\right)\right. \\ & \left. + \left|\mathbf{w}_1^H\mathbf{Z}(n)\right|^2 g'\left(\left|\mathbf{w}_1^H\mathbf{Z}(n)\right|^2\right)\right\}\mathbf{w}_1 \end{aligned} \tag{17}$$

where three versions of the function $g(\bullet)$ are often used: $g_1(t) = \frac{1}{2\sqrt{l_1+t}}$, $g_2(t) = \frac{1}{l_2+t}$, $g_3(t) = t$. $g'(\bullet)$ is the derivative of $g(\bullet)$.

c) Divide $\mathbf{w}_1$ by its norm

$$\mathbf{w}_1 = \frac{\mathbf{w}_1}{\|\mathbf{w}_1\|} \tag{18}$$

Repeat b) and c) until $\mathbf{w}_1$ convergences, and then $\mathbf{w}_2$ is easily obtained through Schmidt orthogonalization, $\mathbf{w}_2 = \mathbf{w}_2 - \mathbf{w}_1\mathbf{w}_1^H\mathbf{w}_2$. After this, the demixing matrix $\mathbf{B}$ is obtained, $\mathbf{B} = \mathbf{W}^H\mathbf{D}^{-\frac{1}{2}}\mathbf{U}^H$, and the source signals can be estimated through (15).

Since $x_{Aux}(n)$ is known, we can calculate the correlation values of $x_{Aux}(n)$ with the two estimated signals to eliminate the permutation ambiguity introduced by the ICA-based separation algorithm. Without of lose generality, we define the estimation of $s(n)$ is $\hat{s}(n) = \mathbf{w}_1^H\mathbf{Z}(n)$, substituting (16) to this equation

$$\begin{aligned} \hat{s}(n) &= \left[\mathbf{B}_{1,1}, \mathbf{B}_{1,2}\right]\mathbf{M}\begin{bmatrix} x_T^{PA}(n) \\ s(n) \end{bmatrix} + \left[\mathbf{B}_{1,1}, \mathbf{B}_{1,2}\right]\begin{bmatrix} \xi(n) \\ n_{ADC}^{Aux}(n) \end{bmatrix} \\ &= \left[\mathbf{B}_{1,1}f_{SI} + \varepsilon\mathbf{B}_{1,2}, \mathbf{B}_{1,1}f_{SOI}\right]\begin{bmatrix} x_T^{PA}(n) \\ s(n) \end{bmatrix} \\ &\quad + \left[\mathbf{B}_{1,1}, \mathbf{B}_{1,2}\right]\begin{bmatrix} \xi(n) \\ n_{ADC}^{Aux}(n) \end{bmatrix} \end{aligned} \tag{19}$$

B. DIGITAL SIC BASED ON ICA FOR BOTH LOS AND NON-LOS COMPONENTS EXISTING IN SI CHANNEL

In this case, the SI and intended multipath channels are modeled as FIR filters. The equation (8) can be rewritten as

$$y(n) = \sqrt{p_{SI}}\mathbf{f}_{SIe}^T\mathbf{x}(n) + \mathbf{f}_{SOI}^T\mathbf{s}(n) + \xi(n) \tag{20}$$

where $\mathbf{f}_{SIe} = [f_{SIe}(0), f_{SIe}(1), \cdots, f_{SIe}(L-1)]^T$, $\mathbf{f}_{SOI} = [f_{SOI}(0), f_{SOI}(1), \cdots, f_{SOI}(L-1)]^T$, L denotes the order of the channel filter and $[\bullet]^T$ denotes the transpose operator. $\mathbf{x}(n) = \left[x_T^{PA}(n), x_T^{PA}(n-1), \cdots, x_T^{PA}(n-L+1)\right]^T$ and $E\left[\left|\mathbf{f}_{SIe}^T\mathbf{x}(n)\right|^2\right] = 1$, $\mathbf{s}(n) = [s(n), s(n-1), \cdots, s(n-L+1)]^T$. According to equation (13) and (20), the received data can be written as

$$\mathbf{R}(n) = \begin{bmatrix} \sqrt{p_{SI}}\mathbf{f}_{SIe}^T\mathbf{x}(n) + \mathbf{f}_{SOI}^T\mathbf{s}(n) \\ \varepsilon x_T^{PA}(n) \end{bmatrix} + \begin{bmatrix} \xi(n) \\ n_{ADC}^{Aux}(n) \end{bmatrix} \quad (21)$$

Considering the definition of $\mathbf{x}(n)$ under equation (20) that $\mathbf{x}(n)$ consists of $x_T^{PA}(n)$ and using the FIR filter $\mathbf{f}_{SIe}$ to filter the auxiliary receiver data, equation (21) can be transformed into

$$\bar{\mathbf{R}}(n) = \begin{bmatrix} \sqrt{p_{SI}}\mathbf{f}_{SIe}^T\mathbf{x}(n) + \mathbf{f}_{SOI}^T\mathbf{s}(n) \\ \varepsilon\mathbf{f}_{SIe}^T\mathbf{x}(n) \end{bmatrix} + \begin{bmatrix} \xi(n) \\ \xi_{Aux}(n) \end{bmatrix} \quad (22)$$

where $\xi_{Aux}(n) = \sum_{l=0}^{L} f_{SIe}(l)\, n_{ADC}^{Aux}(n-l)$. Equation (22) can be rewritten as

$$\bar{\mathbf{R}}(n) = \begin{bmatrix} \sqrt{p_{SI}} & 1 \\ \varepsilon & 0 \end{bmatrix} \begin{bmatrix} \mathbf{f}_{SIe}^T\mathbf{x}(n) \\ \mathbf{f}_{SOI}^T\mathbf{s}(n) \end{bmatrix} + \begin{bmatrix} \xi(n) \\ \xi_{Aux}(n) \end{bmatrix} \quad (23)$$

To note that equation (23) is similar to equation (14). However, it is unavailable to use the method in the subsection III. A directly since the SI channel is unknown. As introduced in subsection III.A, the aim of ICA-based separation method is to search for a demixing matrix $\mathbf{B}$ to make $\mathbf{B}\begin{bmatrix} \sqrt{p_{SI}} & 1 \\ \varepsilon & 0 \end{bmatrix}$ be a generalized permutation matrix. It is easy to obtain that one solution of $\mathbf{B}$ is

$$\mathbf{B} = \begin{bmatrix} 0 & 1 \\ 1 & \beta \end{bmatrix} \quad (24)$$

where $\beta = -\frac{\sqrt{p_{SI}}}{\varepsilon}$. Then, the problem becomes to estimate β and $\mathbf{f}_{SIe}$.

We use the contrast function for the ICA-based separation method in [35]

$$J = E\left\{G\left(\mathbf{B}_{1,:}\bar{\mathbf{R}}(n)\right) + G\left(\mathbf{B}_{2,:}\bar{\mathbf{R}}(n)\right)\right\} \quad (25)$$

where $G(\bullet)$ is a smooth real even function. Maximizing the contrast function and taking the constraint of $\mathbf{f}_{SIe}$ into account, we obtain the following optimization problem:

$$\begin{aligned} &\underset{\beta,\mathbf{f}_{SIe}}{\text{maximize}}\, J = E\left\{G\left(\mathbf{B}_{1,:}\bar{\mathbf{R}}(n)\right) + G\left(\mathbf{B}_{2,:}\bar{\mathbf{R}}(n)\right)\right\} \\ &s.t.\ E\left[\left|\mathbf{f}_{SIe}^T\mathbf{x}(n)\right|^2\right] = 1 \end{aligned} \quad (26)$$

For ease of analysis, we assume $E\left[\mathbf{x}(n)\mathbf{x}^H(n)\right] = \mathbf{I}$ ($[\bullet]^H$ denotes the conjugate transpose operator), and then the constraint in (26) is transformed into $\|\mathbf{f}_{SIe}\|^2 = 1$, where $\|\bullet\|$ denotes the Frobenius norm. We now give the alternative optimization algorithm based on gradient descent for (26):

$$\begin{aligned} \mathbf{f}_{SIe} = \mathbf{f}_{SIe} + \mu_1 E\Big\{&\mathbf{f}_{SIe}^T\mathbf{x}_A(n)\mathbf{x}_A^*(n)\, g\left(\left|\mathbf{f}_{SIe}^T\mathbf{x}_A(n)\right|^2\right) \\ &+ \beta\left(\mathbf{y}(n) + \beta\mathbf{f}_{SIe}^T\mathbf{x}_A(n)\right)\mathbf{x}_A^*(n) \\ &\times g\left(\left|\mathbf{y}(n) + \beta\mathbf{f}_{SIe}^T\mathbf{x}_A(n)\right|^2\right)\Big\} \end{aligned}$$

$$\mathbf{f}_{SIe} = \frac{\mathbf{f}_{SIe}}{\|\mathbf{f}_{SIe}\|} \quad (27)$$

$$\begin{aligned} \beta = \beta + \mu_2 E\Big\{&\mathrm{Re}\left[\mathbf{f}_{SIe}^T\mathbf{x}_A(n)\left(\mathbf{y}(n) + \beta\mathbf{f}_{SIe}^T\mathbf{x}_A(n)\right)^*\right] \\ &\times g\left(\left|\mathbf{y}(n) + \beta\mathbf{f}_{SIe}^T\mathbf{x}_A(n)\right|^2\right)\Big\} \end{aligned} \quad (28)$$

where $\mathbf{x}_A(n) = [x_{Aux}(n), x_{Aux}(n-1), \cdots, x_{Aux}(n-L+1)]^T$ and $g(\bullet)$ is the derivative of $G(\bullet)$. (27) and (28) are calculated alternately until β and $\mathbf{f}_{SIe}$ converge. More details of the derivation can be seen in Appendix A.

Once β and $\mathbf{f}_{SIe}$ are estimated, the residual signal after digital SIC stage can be written as

$$\begin{aligned} \hat{s}(n) = &\left(\sqrt{p_{SI}}\mathbf{f}_{SIe}^T + \beta\hat{\mathbf{f}}_{SIe}^T\right)\mathbf{x}(n) + \mathbf{f}_{SOI}^T\mathbf{s}(n) \\ &+ \xi(n) + \beta\xi_{Aux}(n) \end{aligned} \quad (29)$$

where $\hat{\mathbf{f}}_{SIe}$ is the estimation of $\mathbf{f}_{SIe}$.

IV. SIMULATION AND RESULTS

In this section, the validity of the above two proposed digital SIC schemes is verified by numerical simulations. We consider a CCFD communication system with two users communicating with each other through QPSK signal. A complete transmit chain is implemented to model the conduct of the PA, LNA, AGC and ADC. We compare the performance of the proposed algorithms with LS estimators for the two CCFD communication scenarios. In the simulations, all channel taps are generated as complex zero-mean independent and identically distributed Gaussian random variables and all statistics are evaluated over 500 Mont-Carlo runs. If not specifically stated below, the simulation parameters are set as ADC input SNR=20dB, PAPR=10dB, and sample length N=5000. For brevity, we define the SI only has LOS component as Channel.1 and define the SI has LOS and non-LOS components as Channel.2.

Fig.3 shows the performance of the proposed system schemes for different number of bits at ADC. It can be seen from Fig.3 (a) that the number of bits at ADC has little effect on the interference cancellation and the proposed method with nonlinear function g_2 and g_3 outperform LS-based method around 4dB in SIC capacity. To explain these phenomenon, noting that the quantization noise to signal ratio at auxiliary receive chain is very low (i.e., the digital baseband signal $x_{Aux}(n)$ is almost pure), and combining the desired signal and noise at ordinary receive chain as a new signal, (14) can be treated as noiseless mixture model. In addition, the separation performance of ICA-based BSS algorithm is

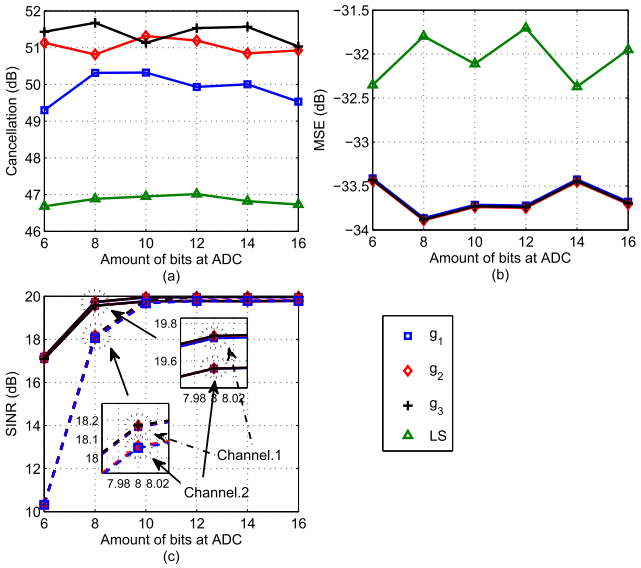

FIGURE 3. Performance of the proposed ICA-based digital SIC schemes for different amount of bits at ADC. a) amount of cancellation versus number of bits at ADC for Channel.1, input SIR=−10dB; b) mean square error of the SI channel estimation versus amount of bits at ADC for Channel.2, input SIR=−10dB, channel order L=3; c) output SINR versus amount of bits at ADC, solid line for input SIR=-10dB and dash line for input SIR=−20dB.

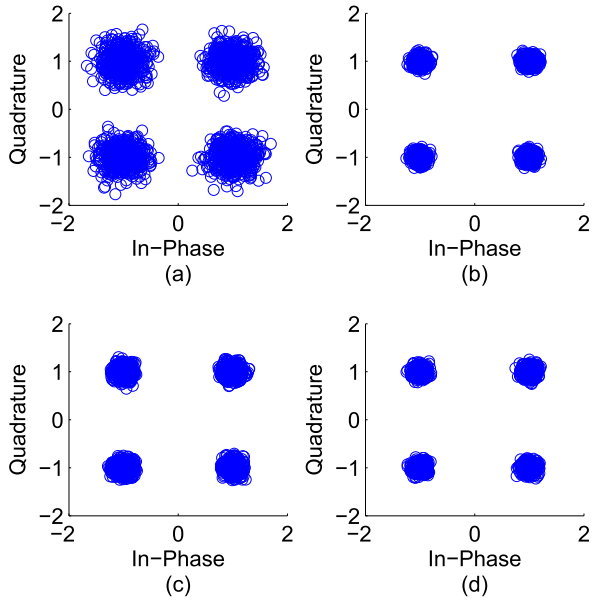

FIGURE 4. The constellation results of proposed method for Channel 1 when SNR=20dB at the input of ADC. (a) input SIR=−20dB, the quantization bits number is 6; (b) input SIR=−20dB, the quantization bits number is 14; (c) input SIR=−10dB, the quantization bits number is 6; (d) input SIR=−10dB, the quantization bits number is 14.

not sensitive to input SIR. So, the quantization bits number has little effect on SIC. Fig.3 (b) shows the mean square error (MSE) of the SI channel estimation versus number of bits at ADC. In ground communication systems, the number of main paths is around 3-6, and we select as 3 in this paper. The proposed method with the three nonlinear functions have a similar MSE performance and are better than that of LS-based method. Fig.3 (c) shows the performance of output

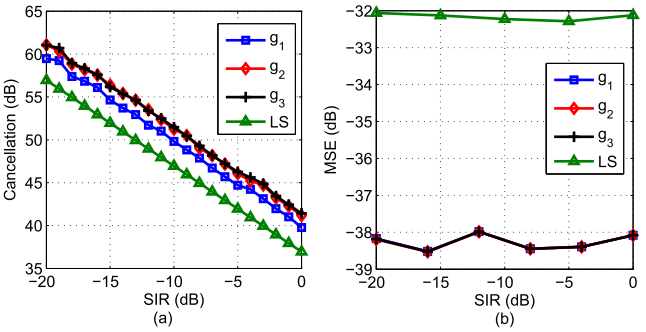

FIGURE 5. Performance of the proposed ICA-based digital SIC schemes for different input SIR. a) amount of cancellation versus input SIR for Channel.1, the number of quantization bit is 14; b) mean square error of the SI channel estimation versus input SIR for Channel.2, the number of quantization bit is 14, channel order L=3.

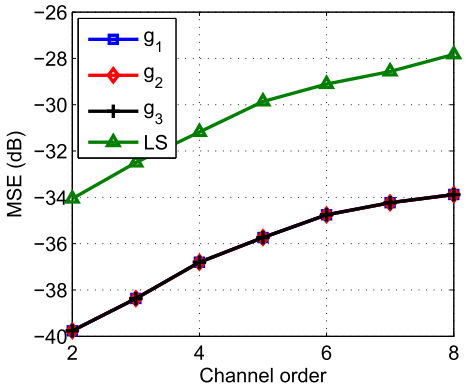

FIGURE 6. Mean square error of the SI channel estimation versus channel order of the proposed ICA-based digital SIC scheme for different channel order, the number of quantization bits is 14, input SIR=−10dB.

SINR for different number of bits at ADC and we have considered two cases for both Channel.1 and Chennel.2 in which the residual SIR after RF SIC stage (i.e., the input SIR at digital SIC stage) are −10 dB and −20dB. We can observe that the output SINR heavily relies on the number of quantization bit of ADC, the output SINR increases fast when the number of bits at ADC is low and saturates as the quantization bits keeps increasing. The reason is that the main factor limiting the system performance is the quantization error when the quantization bit number is low. As the quantization bit number increases (i.e., the precision of ADC increases), the impact of ADC decreases and other effects will become the bottleneck. Fig. 4 shows the constellation results of proposed method for Channel 1 at different simulation conditions. It can be seen that the impact of the quantization bits number at low input SIR is much higher than that at high input SIR. Fig. 3 also shows that when input SIR increases from −20dB to −10dB, the quantization bits required in ADC can be decreased by 3 bits to obtain the same SINR value.

Fig. 5 shows the performance of the proposed system schemes for different input SIR. From Fig. 5 (a), we can observe that the amount of SIC in dB scale for Channel.1 decreases almost linearly with the input SIR and

the proposed method with nonlinear function g_2 and g_3 outperform LS-based method around 5dB in SIC capacity. It indicates that the output SIR is maintained at a certain level and independent of the input SIR. Fig. 5 (b) shows that the MSE performance of the proposed algorithm for Channel.2 is not sensitive to the input SIR and the proposed method with the three nonlinear functions have a similar MSE performance with around 6dB gains compared with LS-based method.

The performance of the proposed digital SIC algorithm for different channel order of Channel.2 is presented in Fig. 6. Fig. 6 reveals that the MSE increases with the channel order. The proposed method with the three nonlinear functions have a similar performance and outperform LS-based method around 6dB.

V. CONCLUSION

In this paper, two digital baseband SIC algorithms based on the concept of ICA have been proposed. The first algorithm solves the case when SI only has LOS component. In the second algorithm, the SIC problem with multipath SI channel is solved. Both of the two proposed algorithms take the output signal at PA in transmit chain as the reference signal for both RF and digital baseband SIC stages. Consequently, all the nonlinear factors introduced by transmitter would not impact on the SIC at receiver. At receiver, the effect of ADC is also considered. The proposed two approaches are evaluated by simulation, and the simulation results show that the proposed methods improve the channel estimation accuracy and the SIC performance.

APPENDIX

We shall derive the alternative optimization algorithm based on gradient descent for (26). Let $\mathbf{f}_{SIe}(n) = \mathbf{f}^r_{SIe}(n) + i\mathbf{f}^i_{SIe}(n)$. For the ease of derivations, the algorithm updates the real and imaginary parts of $\mathbf{f}_{SIe}(n)$ separately. For briefly, the time index is omitted in the following without ambiguity. The optimization problem of (26) can be rewritten as

$$\begin{aligned} &\underset{\beta,\mathbf{f}_{SIe}}{\text{maximize}}\, J = E\left\{G\left(\left|\mathbf{f}_{SIe}^T\mathbf{x}_A\right|^2\right) + G\left(\left|y+\beta\mathbf{f}_{SIe}^T\mathbf{x}_A\right|^2\right)\right\} \\ &s.t.\quad \|\mathbf{f}_{SIe}\| = 1 \end{aligned} \tag{30}$$

The derivative of the contrast with respect to $\mathbf{f}_{SIe}$ is

$$\nabla_f J = \nabla_f E\left\{G\left(\left|\mathbf{f}_{SIe}^T\mathbf{x}_A\right|^2\right)\right\} + \nabla_f E\left\{G\left(\left|y+\beta\mathbf{f}_{SIe}^T\mathbf{x}_A\right|^2\right)\right\} \tag{31}$$

where the gradient is computed with respect to the real and imaginary parts of $\mathbf{f}_{SIe}$ separately. The first and second terms of the right hand in (31) are (32) and (33), as shown at the bottom of this page, respectively.

$$\nabla_f E\left\{G\left(\left|\mathbf{f}_{SIe}^T\mathbf{x}_A\right|^2\right)\right\} = \begin{pmatrix} \frac{\partial}{\partial \mathbf{f}^r_{SIe}(0)} \\ \frac{\partial}{\partial \mathbf{f}^i_{SIe}(0)} \\ \vdots \\ \frac{\partial}{\partial \mathbf{f}^r_{SIe}(L-1)} \\ \frac{\partial}{\partial \mathbf{f}^i_{SIe}(L-1)} \end{pmatrix} E\left\{G\left(\left|\mathbf{f}_{SIe}^T\mathbf{x}_A\right|^2\right)\right\} = 2\begin{pmatrix} E\left\{\mathrm{Re}\left[\mathbf{f}_{SIe}^T\mathbf{x}_A\mathbf{x}_{A1}^*\right]g\left(\left|\mathbf{f}_{SIe}^T\mathbf{x}_A\right|^2\right)\right\} \\ E\left\{\mathrm{Im}\left[\mathbf{f}_{SIe}^T\mathbf{x}_A\mathbf{x}_{A1}^*\right]g\left(\left|\mathbf{f}_{SIe}^T\mathbf{x}_A\right|^2\right)\right\} \\ \vdots \\ E\left\{\mathrm{Re}\left[\mathbf{f}_{SIe}^T\mathbf{x}_A\mathbf{x}_{AL}^*\right]g\left(\left|\mathbf{f}_{SIe}^T\mathbf{x}_A\right|^2\right)\right\} \\ E\left\{\mathrm{Im}\left[\mathbf{f}_{SIe}^T\mathbf{x}_A\mathbf{x}_{AL}^*\right]g\left(\left|\mathbf{f}_{SIe}^T\mathbf{x}_A\right|^2\right)\right\} \end{pmatrix} \tag{32}$$

$$\begin{aligned} \nabla_f E\left\{G\left(\left|y+\beta\mathbf{f}_{SIe}^T\mathbf{x}_A\right|^2\right)\right\} &= \begin{pmatrix} \frac{\partial}{\partial \mathbf{f}^r_{SIe}(0)} \\ \frac{\partial}{\partial \mathbf{f}^i_{SIe}(0)} \\ \vdots \\ \frac{\partial}{\partial \mathbf{f}^r_{SIe}(L-1)} \\ \frac{\partial}{\partial \mathbf{f}^i_{SIe}(L-1)} \end{pmatrix} E\left\{G\left(\left|y+\beta\mathbf{f}_{SIe}^T\mathbf{x}_A\right|^2\right)\right\} \\ &= 2\beta\begin{pmatrix} E\left\{\mathrm{Re}\left[\left(y+\beta\mathbf{f}_{SIe}^T\mathbf{x}_A\right)\mathbf{x}_{A1}^*\right]g\left(\left|y+\beta\mathbf{f}_{SIe}^T\mathbf{x}_A\right|^2\right)\right\} \\ E\left\{\mathrm{Im}\left[\left(y+\beta\mathbf{f}_{SIe}^T\mathbf{x}_A\right)\mathbf{x}_{A1}^*\right]g\left(\left|y+\beta\mathbf{f}_{SIe}^T\mathbf{x}_A\right|^2\right)\right\} \\ \vdots \\ E\left\{\mathrm{Re}\left[\left(y+\beta\mathbf{f}_{SIe}^T\mathbf{x}_A\right)\mathbf{x}_{AL}^*\right]g\left(\left|y+\beta\mathbf{f}_{SIe}^T\mathbf{x}_A\right|^2\right)\right\} \\ E\left\{\mathrm{Im}\left[\left(y+\beta\mathbf{f}_{SIe}^T\mathbf{x}_A\right)\mathbf{x}_{AL}^*\right]g\left(\left|y+\beta\mathbf{f}_{SIe}^T\mathbf{x}_A\right|^2\right)\right\} \end{pmatrix} \end{aligned} \tag{33}$$

Given β, the update of $\mathbf{f}_{SIe}$ based on gradient descent is

$$\begin{aligned}\mathbf{f}_{SIe} &= \mathbf{f}_{SIe} + \mu_1 \nabla_f J \\ &= \mathbf{f}_{SIe} + \mu_1 E\left\{\mathbf{f}_{SIe}^T \mathbf{x}_A \mathbf{x}_A^* g\left(\left|\mathbf{f}_{SIe}^T \mathbf{x}_A\right|^2\right)\right. \\ &\quad \left. + \beta\left(y + \beta \mathbf{f}_{SIe}^T \mathbf{x}_A\right)\mathbf{x}_A^* g\left(\left|y + \beta \mathbf{f}_{SIe}^T \mathbf{x}_A\right|^2\right)\right\} \\ \mathbf{f}_{SIe} &= \frac{\mathbf{f}_{SIe}}{\|\mathbf{f}_{SIe}\|} \end{aligned} \tag{34}$$

where μ_1 is convergence factor.

The derivative of the contrast with respect to β is

$$\begin{aligned}\nabla_\beta J &= \nabla_\beta E\left\{G\left(\left|y + \beta \mathbf{f}_{SIe}^T \mathbf{x}_A\right|^2\right)\right\} \\ &= 2\beta E\left\{\left(y + \beta \mathbf{f}_{SIe}^T \mathbf{x}_A\right)\mathbf{x}_A^* g\left(\left|y + \beta \mathbf{f}_{SIe}^T \mathbf{x}_A\right|^2\right)\right\}\end{aligned} \tag{35}$$

Given $\mathbf{f}_{SIe}$, the update of β based on gradient descent is

$$\begin{aligned}\beta &= \beta + \mu_2 \nabla_\beta J \\ &= \beta + \mu_2 E\left\{\beta\left(y + \beta \mathbf{f}_{SIe}^T \mathbf{x}_A\right)\mathbf{x}_A^* g\left(\left|y + \beta \mathbf{f}_{SIe}^T \mathbf{x}_A\right|^2\right)\right\}\end{aligned} \tag{36}$$

where μ_1 is convergence factor. The optimization problem of (26) can be solved through calculating (34) and (36) alternately until $\mathbf{f}_{SIe}$ and β converge.

ACKNOWLEDGEMENT

The authors would like to thank the anonymous reviewers and the editors for helping improve this work.

REFERENCES

[1] A. Goldsmith, *Wireless Communication*, Cambridge, U.K.: Cambridge Univ. Press, 2005.
[2] S. Hong *et al.*, "Applications of self-interference cancellation in 5G and beyond," *IEEE Commun. Mag.*, vol. 52, no. 2, pp. 114–121, Feb. 2014.
[3] Z. Zhang, X. Chai, K. Long, A. V. Vasilakos, and L. Hanzo, "Full duplex techniques for 5G networks: Self-interference cancellation, protocol design, and relay selection," *IEEE Commun. Mag.*, vol. 53, no. 5, pp. 128–137, May 2015.
[4] L. Wang, F. Tian, T. Svensson, D. Q. Feng, M. Song, and S. Q. Li, "Exploiting full duplex for device-to-device communications in heterogeneous networks," *IEEE Commun. Mag.*, vol. 53, no. 5, pp. 146–152, May 2015.
[5] Y. Liao, L. Y. Song, Z. Han, and Y. H. Li, "Full duplex cognitive radio: A new design paradigm for enhancing spectrum usage," *IEEE Commun. Mag.*, vol. 53, no. 5, pp. 138–145, May 2015.
[6] D. Korpi *et al.*, "Full-duplex mobile device: Pushing the limits," *IEEE Commun. Mag.*, vol. 54, no. 9, pp. 80–87, Sep. 2016.
[7] E. Ahmed and A. M. Eltawil, "All-digital self-interference cancellation technique for full-duplex systems," *IEEE Trans. Wireless Commun.*, vol. 14, no. 7, pp. 3519–3532, Jul. 2015.
[8] M. Heino *et al.*, "Recent advances in antenna design and interference cancellation algorithms for in-band full duplex relays," *IEEE Commun. Mag.*, vol. 53, no. 5, pp. 91–101, May 2015.
[9] M. K. Chung, M. S. Sim, J. Kim, D. K. Kim, and C.-B. Chae, "Prototyping real-time full duplex radios," *IEEE Commun. Mag.*, vol. 53, no. 9, pp. 56–63, Sep. 2015.
[10] M. Jain *et al.*, "Practical, real-time, full duplex wireless," in *Proc. MobiCom*, Las Vegas, NV, USA, Sep. 2011, pp. 301–312.
[11] M. Duarte and A. Sabharwal, "Full-duplex wireless communications using off-the-shelf radios: Feasibility and first results," in *Proc. Asilomar Conf. Signals, Syst. Comput.*, Pacific Grove, CA, USA, Nov. 2010, pp. 1558–1562.
[12] E. Everett, A. Sahai, and A. Sabharwal, "Passive self-interference suppression for full-duplex infrastructure nodes," *IEEE Trans. Wireless Commun.*, vol. 13, no. 2, pp. 680–694, Jan. 2014.
[13] S. Maddio, A. Cidronali, and G. Manes, "Real-time adaptive transmitter leakage cancelling in 5.8-GHz full-duplex transceivers," *IEEE Trans. Microw. Theory Techn.*, vol. 63, no. 2, pp. 509–519, Feb. 2015.
[14] S. Maddio, A. Cidronali, and G. Collodi, "Base-band training of carrier leakage canceller in 5.8-GHz full-duplex transceivers," *Microw. Opt. Technol. Lett.*, vol. 58, no. 11, pp. 2649–2653, 2016.
[15] A. Sabharwal, P. Schniter, D. Guo, D. W. Bliss, S. Rangarajan, and R. Wichman, "In-band full-duplex wireless: Challenges and opportunities," *IEEE J. Sel. Areas Commun.*, vol. 32, no. 9, pp. 1637–1652, Sep. 2014.
[16] J. Wang, Z. H. Zhao, C. J. Qing, and Y. X. Tang, "Adaptive self-interference cancellation at RF domain in co-frequency co-time full duplex systems," (in Chinese), *J. Elect. Inf. Technol.*, vol. 36, no. 6, pp. 1435–1440, 2014.
[17] Q. Xu, X. Quan, W. S. Pan, S. H. Shao, and Y. X. Tang, "Analysis and experimental verification of RF self-interference cancelation for co-time co-frequency full-duplex LTE," (in Chinese), *J. Electr. Inf. Technol.*, vol. 36, no. 3, pp. 662–668, 2014.
[18] Z. He, S. Shao, Y. Shen, C. Qing, and Y. Tang, "Performance analysis of RF self-interference cancellation in full-duplex wireless communications," *IEEE Wireless Commun. Lett.*, vol. 3, no. 4, pp. 405–408, Aug. 2014.
[19] B. Kaufman, J. Lilleberg, and B. Aazhang, "An analog baseband approach for designing full-duplex radios," in *Proc. IEEE Signals, Syst. Comput. Asilomar Conf.*, Sep. 2013, pp. 987–991.
[20] V. Syrjala, M. Valkama, L. Anttila, T. Riihonen, and D. Korpi, "Analysis of oscillator phase-noise effects on self-interference cancellation in full-duplex OFDM radio transceivers," *IEEE Trans. Wireless Commun.*, vol. 13, no. 6, pp. 2977–2990, Jun. 2014.
[21] D. Korpi, L. Anttila, V. Syrjala, and M. Valkama, "Widely linear digital self-interference cancellation in direct-conversion full-duplex transceiver," *IEEE J. Sel. Areas Commun.*, vol. 32, no. 9, pp. 1674–1687, Sep. 2014.
[22] S. H. Li and R. D. Murch, "An investigation into baseband techniques for single-channel full-duplex wireless communication systems," *IEEE Trans. Wireless Commun.*, vol. 13, no. 9, pp. 4794–4806, Sep. 2014.
[23] M. Duarte, C. Dick, and A. Sabharwal, "Experiment-driven characterization of full-duplex wireless systems," *IEEE Trans. Wireless Commun.*, vol. 11, no. 12, pp. 4296–4307, Dec. 2012.
[24] S. Li and R. D. Murch, "Full-duplex wireless communication using transmitter output based echo cancellation," in *Proc. IEEE Global Telecommun. Conf.*, Sep. 2011, pp. 1–5.
[25] E. Ahmed, A. Eltawil, and A. Sabharwal, "Self-interference cancellation with phase noise induced ICI suppression for full-duplex systems," in *Proc. GLOBECOM*, Dec. 2013, pp. 3384–3388.
[26] G. Zheng, I. Krikidis, and B. Ottersten, "Full-duplex cooperative cognitive radio with transmit imperfections," *IEEE Trans. Wireless Commun.*, vol. 12, no. 5, pp. 2498–2511, May 2013.
[27] A. Masmoudi and T. Le-Ngoc, "A maximum-likelihood channel estimator for self-interference cancelation in full-duplex systems," *IEEE Trans. Veh. Technol.*, vol. 65, no. 7, pp. 5122–5132, Sep. 2016.
[28] V. Syrjala, K. Yamamoto, and M. Valkama, "Analysis and design specifications for full-duplex radio transceivers under RF oscillator phase noise with arbitrary spectral shape," *IEEE Trans. Veh. Technol.*, vol. 65, no. 8, pp. 6782–6788, Aug. 2016.
[29] D. Korpi, T. Riihonen, V. Syrjala, L. Anttila, M. Valkama, and R. Wichman, "Full-duplex transceiver system calculations: Analysis of ADC and linearity challenges," *IEEE Trans. Wireless Commun.*, vol. 13, no. 7, pp. 3821–3836, Jul. 2014.
[30] D. Bharadia, E. McMilin, and S. Katti, "Full duplex radios," in *Proc. SIGCOMM*, Aug. 2013, pp. 375–386.
[31] E. Ahmed, A. Eltawil, and A. Sabharwal, "Self-interference cancellation with nonlinear distortion suppression for full-duplex systems," in *Proc. 47th Asilomar Conf. Signals, Syst. Comput.*, Nov. 2013, pp. 1–5.
[32] D. Korpi *et al.*, "Advanced self-interference cancellation and multi-antenna techniques for full-duplex radios," in *Proc. 47th Asilomar Conf. Signals, Syst. Comput.*, Nov. 2013, pp. 1–5. [Online]. Available: http://arxiv.org/abs/1401.3331
[33] J. F. Cardoso, "Blind signal separation: Statistical principles," in *Proc. Ica*, 1998, pp. 78–81.
[34] K. Abed-Meraim, Y. Xiang, J. Manton, and Y. Hua, "Blind source-separation using second-order cyclostationary statistics," *IEEE Trans Signal Process.*, vol. 49, no. 3, pp. 694–701, Mar. 2001.

[35] E. Bingham and A. Hyvarinen, "A fast fixed-point algorithm for independent component analysis of complex valued signals," *Int. J. Neural Syst.*, vol. 10, no. 1, pp. 1–8, 2000.
[36] P. Comon, "Independent component analysis, A new concept?" *Signal Process.*, vol. 36, no. 3, pp. 287–314, 1994.
[37] L. Anttila, "Digital front-end signal processing with widely-linear signal models in radio devices," M.S. thesis, Dept. Commun. Eng., Tampere Univ. Technol., Tampere, Finland, 2011.
[38] Z. Z. Zou, S. X. Zeng, P. Chen, and X. T. Yu, "I/Q imbalance calibration in wideband direct conversion receivers," in *Proc. IEEE Int. Conf. Ubiquitous Wireless Broadband (ICUWB)*, Sep. 2016, pp. 1–4.
[39] T. Schenk, *RF Imperfections in High-Rate Wireless Systems, Impact and Digital Compensation*. New York, NY, USA: Springer-Verlag, 2008.
[40] B. Razavi, *Design of Analog CMOS Integrated Circuits*. New York, NY, USA: McGraw-Hill, 2001.
[41] D. R. Morgan, Z. Ma, J. Kim, M. G. Zierdt, and J. Pastalan, "A generalized memory polynomial model for digital predistortion of RF power amplifiers," *IEEE Trans. Signal Process.*, vol. 54, no. 10, pp. 3852–3860, Oct. 2006.
[42] H. Z. Zhao, J. Wang, and Y. X. Tang, "Performance analysis of RF self-interference cancellation in broadband full duplex systems," in *Proc. IEEE Int. Conf. Commun. Workshops (ICC)*, May 2016, pp. 175–179.
[43] Q. Gu, *RF System Design of Transceivers for Wireless Communications*. New York, NJ, USA: Springer-Verlag, 2006.

JIONG LI (SM'15) received the B.S. degree in communications engineering from the Ocean University of China, Qingdao, China, in 2011, and the M.S. degree in communications engineering from the PLA University of Science and Technology, Nanjing, China, in 2014. He is currently pursuing the Ph.D. degree in information and communications engineering with the College of Communications Engineering, PLA University of Science and Technology. His current research interests include 5G self-interference cancellation, signal processing in communications, and blind source separation.

HANG ZHANG (M'12) received the M.S. degree from Southeast University, Nanjing, China, in 1989 and the B.S. degree from the PLA University of Science and Technology, Nanjing, in 1984. She is currently a Professor and also the Ph.D. Supervisor with the PLA University of Science and Technology. Her research interests include wireless communication, satellite communication, and signal processing in communications.

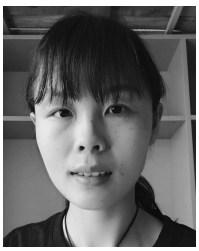

MENGLAN FAN (M'15) received the B.S. degree in communications engineering from the PLA University of Science and Technology, Nanjing, China, in 2014, where she is currently pursuing the M.S. degree in information and communications engineering with the College of Communications Engineering. Her current research interests include cognitive radio technology, green communications, and blind source separation.